



# The mechanism of ceria slurry on chemical mechanical polishing efficiency and surface quality of Gallium nitride

Wenhai Xian<sup>a,b</sup>, Baoguo Zhang<sup>a,b,\*</sup>, Shitong Liu<sup>a,b</sup>, Yijun Wang<sup>a,b</sup>, Sihui Qin<sup>a,b</sup>, Yang Liu<sup>a,b</sup>

<sup>a</sup> School of Electronic Information Engineering, Hebei University of Technology, Tianjin, 300130, People's Republic of China

<sup>b</sup> Tianjin Key Laboratory of Electronic Materials and Devices, Tianjin, 300130, People's Republic of China



## ARTICLE INFO

### Keywords:

Gallium nitride  
Ultra-smooth surface  
Ceria  
Alumina  
Chemical mechanical polishing

## ABSTRACT

The study compares the material removal rate (MRR) and surface roughness of GaN polished with three different abrasives (silica, alumina, and ceria). The findings reveal that CeO<sub>2</sub>-based slurry exhibits the highest MRR of 265.3 nm/h and the lowest surface roughness ( $S_q = 0.075 \text{ nm}$ ), demonstrating its superior performance. Furthermore, the study delves into the mechanisms responsible for the enhanced CMP performance, ascribing it to the robust frictional interaction and heat generation during polishing, which facilitate the oxidation of GaN and subsequent material removal. This investigation offers valuable insights into optimizing CMP processes for GaN-based devices.

## 1. Introduction

Gallium nitride (GaN), when grown on sapphire or silicon substrates, represents an outstanding semiconductor material for the construction of optoelectronic detection devices and high-power lasers. Its unique properties, including a larger bandgap and high electron mobility, render GaN highly promising in the production of high-temperature, high-frequency, and high-power optoelectronic devices, as evidenced in numerous studies [1–6]. In the context of GaN thin films, surface defects can act as recombination centers for charge carriers, significantly diminishing the efficiency of GaN-based devices. Consequently, achieving a smooth and flat surface on GaN thin films is crucial for enhancing the performance of subsequent devices [7]. To address this challenge, Bohan Guo et al. have employed both inductively coupled plasma (ICP) dry etching and chemical mechanical polishing (CMP) techniques for processing GaN samples. Their findings reveal that CMP is capable of mitigating damage caused by ion bombardment, ultimately yielding GaN materials with superior surface quality. Furthermore, experimental data indicates that devices fabricated using CMP-treated GaN materials exhibit improved performance, underscoring the effectiveness of this approach [8].

CMP, an economical and efficient processing method is widely regarded as an indispensable approach for producing GaN thin films with exceptional surface quality. Nonetheless, the pursuit of novel

polishing methodologies to efficiently fabricate GaN materials with superior surface qualities remains an active area of research among scholars. In this context, Li-Wei Ou and his colleagues achieved notable advancements by incorporating a UV-assisted oxidation method during CMP. This modification increased the removal rate of colloidal silica on GaN up to 254.7 nm/h while attaining a minimal roughness (Ra) of 0.76 nm [9]. Similarly, the team at Hebei University of Technology introduced a photocatalyst into the photochemical mechanical polishing process, which significantly bolstered the oxidizing capability of the slurry. This led to an impressive increase in the MRR to 487.9 nm/h. However, the resulting surface quality of the GaN, as indicated by a root mean square roughness (Rq) of 4.24 nm, fell short of optimal standards [10].

Furthermore, there have been endeavors to increase the removal rate of GaN by strengthening the oxidizing power of the colloidal silica slurry. For example, Zifeng Ni et al. successfully augmented the MRR to 274.4 nm/h by employing the electro-Fenton process [11]. Qiongbin Zheng et al. enhanced the oxidizing prowess of the slurry by integrating potassium permanganate (KMnO<sub>8</sub>), a potent oxidizing agent, with electrochemical catalysis, thereby improving the overall performance [12]. Their findings underscore the limitation of excessively robust oxidation in attaining atomically smooth GaN surfaces within a colloidal silica system. Congming Ke et al. achieved a notable MRR of 304.2 nm/h with an alumina polishing film fortified by potassium persulfate

\* Corresponding author. School of Electronic Information Engineering, Hebei University of Technology, Tianjin, 300130, People's Republic of China.  
E-mail address: [bgzhang@hebut.edu.cn](mailto:bgzhang@hebut.edu.cn) (B. Zhang).

**Table 1**  
Hardness of abrasives [18].

Name	Value (Mohs)
SiO <sub>2</sub>	7
Al <sub>2</sub> O <sub>3</sub>	9
CeO <sub>2</sub>	5–6

(K<sub>2</sub>S<sub>2</sub>O<sub>8</sub>), while minimizing the surface roughness (Ra) to 0.42 nm [13]. Qiubo Li's team executed CMP on GaN utilizing a blend of zirconia (ZrO<sub>2</sub>) and silica (SiO<sub>2</sub>) abrasives under weak alkaline conditions. This approach yielded an exceptional GaN surface quality with Ra of 0.059 nm, which is close to the theoretical roughness limit of GaN. However, the MRR peaked at 89.05 nm/h, leaving a room for improvement in polishing efficiency [14]. Their study shows that the abrasive type may have an effect on planarization of GaN thin films. Recent investigations have confirmed that the frictional interaction between the abrasive and GaN surface during CMP directly modulates the GaN removal rate, and that the synergy between mechanical abrasion and oxidation enhances the post-polishing surface quality of GaN [15,16]. The research of Huaijun Guan et al. highlights that, within a given abrasive system, a lower coefficient of friction (COF) between the polishing slurry and GaN correlates positively with superior CMP-treated GaN surface quality. Conversely, a high COF leads to a more pronounced MRR [17].

Because of the limited CMP efficiency in polishing GaN with colloidal silica slurry, the present study endeavors to address this challenge by conducting a polishing experiment on 4-inch GaN films, employing three distinct abrasives with varying degrees of hardness and morphological characteristics. This study presents a significant advancement in the GaN CMP by utilizing ceria-based slurry, which achieves the highest MRR of 265.3 nm/h and the lowest surface roughness (Sq = 0.075 nm). The investigation delves into the mechanisms behind the improved CMP performance, emphasizing the synergistic effects of frictional interaction and thermally accelerated oxidation, which facilitate the efficient removal of oxide layers without causing damage to the underlying GaN surface. This research not only highlights the optimal abrasive (ceria) for ultra-smooth GaN surfaces but also provides valuable insights into enhancing the CMP process for GaN-based devices.

## 2. Materials and methods

### 2.1. Materials

The wafers employed in the CMP experiments consisted of 4-inch GaN films, with a film thickness of  $3.5 \pm 0.5$   $\mu\text{m}$ , grown atop a sapphire substrate utilizing the Hydride Vapor Phase Epitaxy (HVPE) technique. The basic constituents of the slurry consisted of abrasives, oxidants, pH regulators, and deionized water. This particular study selected three distinct abrasives: colloidal silica with a mean diameter of 110 nm, alumina ( $\text{Al}_2\text{O}_3$ ) powder with an original mean diameter of 11.5  $\mu\text{m}$ , and ceria ( $\text{CeO}_2$ ) powder with an original mean diameter of 2.3  $\mu\text{m}$ . The Mohs hardness values of these three abrasives are listed in

**Table 1.** The oxidant utilized was potassium persulphate (K<sub>2</sub>S<sub>2</sub>O<sub>8</sub>) of analytical reagent (AR) grade, while the pH regulators consisted of nitric acid (HNO<sub>3</sub>, AR grade) and potassium hydroxide (KOH, AR grade).

### 2.2. Preparation of the different slurry

The colloidal silica-based slurry required for this study was obtained by diluting the original colloidal silica according to a certain ratio, adding K<sub>2</sub>S<sub>2</sub>O<sub>8</sub>, and adjusting the pH to 3.0 with HNO<sub>3</sub>. Alumina and ceria polishing slurries were prepared using the high-energy ball milling (HEBM) method. The ball milling equipment used in this study was a planetary ball mill, the schematic diagram of the ball milling equipment is shown in Fig. 1 and the parameters of the equipment and ball milling additives are shown in Table 2. The zirconia beads in the ball milling slurry were filtered out after it was finished to obtain the original

**Table 2**  
Parameters of equipment and ball milling additives.

Parameter	Condition
Power material	$\text{Al}_2\text{O}_3$ or $\text{CeO}_2$
Initial power mass	60 g
pH of ball milling solution	3
DI water mass	240 g
Grinding ball material	Zirconium beads (Dia.: 0.6–0.8 mm)
Ball-to-powder weight ratio	4:1
Rotation Speed	700 rpm
Total milling time	2 h
Ball milling jar	Polyamide 66
Types of milling	Wet

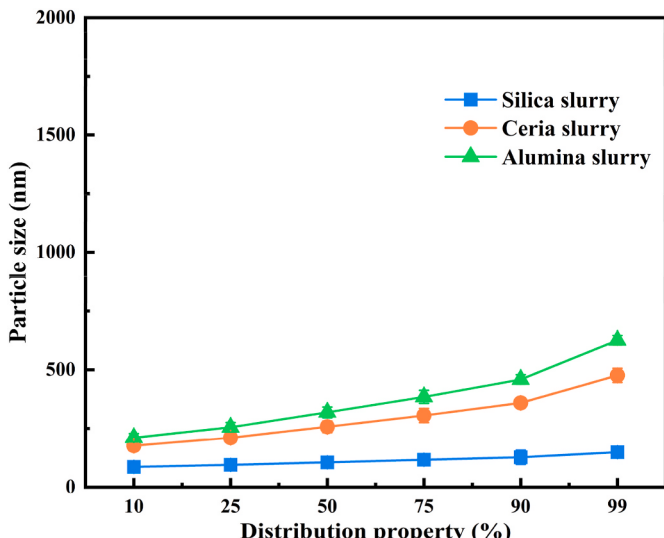


Fig. 2. Particle size distribution of the three original polishing slurries.

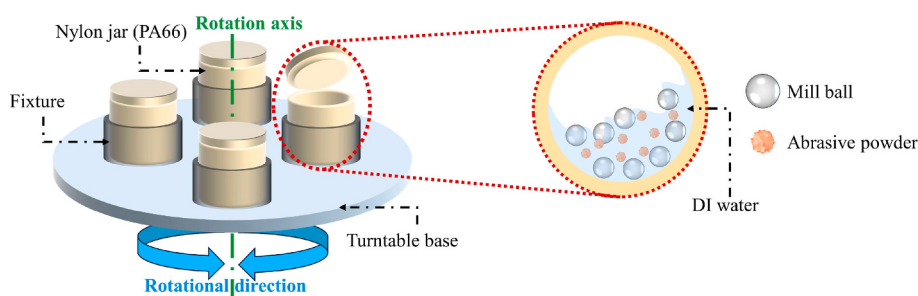


Fig. 1. Schematic diagram of planetary ball mill machine.

**Table 3**  
Parameters of the polisher.

Parameter	Unit	Value
Polishing pressure	psi	5.8
Polishing time	min	30
Slurry flow rate	ml/min	80
Pad rotation speed	rpm	50
Head rotation speed	rpm	50

alumina and ceria slurries, both with an abrasive concentration of 20.0 wt%. In the CMP experiment, the two original slurries were diluted in a certain ratio,  $K_2S_2O_8$  was added and the pH was adjusted with  $HNO_3$  to prepare the alumina and ceria slurries required for the study. The concentration of  $K_2S_2O_8$  in all the slurries was kept as 2.0 wt% and the pH was 3.0. The particle size distribution (D10 to D99) in the colloidal silica and ball-milled alumina and ceria original slurries is shown in Fig. 2 [19–21]. In this study, the abrasive particles larger than 500 nm were eliminated to minimize experimental errors caused by large particles.

### 2.3. CMP experiments

All CMP experiments in this study were performed in a polisher (SSP500, manufactured by Wuxi RX Lapping & Polishing Technology Corporation, China) with a polyurethane polishing pad. The type of polishing pad was Suba 600. The specific parameter settings of the polisher are shown in Table 3. Each CMP experiment was repeated three times, and the MRR was calculated by measuring the change in the average thickness of the film, which was calculated as shown in Eq. (1):

$$MRR = \frac{h_0 - h_1}{t} \quad (1)$$

where,  $h_0$  (nm) is the initial mean thickness of the GaN film before polishing, and  $h_1$  (nm) is the mean thickness of the GaN film after polishing.  $t$  is the time of the polishing process. The average of the calculated results is taken as the reference value and the range as the error [22,23].

### 2.4. Characterization techniques

The LPSA (NICOMP380ZLS; manufactured by Particle Sizing Systems Inc., U.S.A.) was utilized to determine the particle size distribution of the slurries through the dynamic light scattering (DLS) technique. The surface roughness ( $S_q$ ,  $100 \mu m^2$ ) of the polished GaN films was

quantified using an atomic force microscope (AFM), with the surface morphology characteristics observed during the process. The AFM data was subsequently analyzed in detail for defect study by the software "Gwyddion" to extract peak-to-valley (P-V) values within the measurement range. The microscopic morphology of the three abrasives and the post-polishing surface characteristics of the GaN films were investigated using scanning electron microscopy (SEM; Sigma 500). Furthermore, the elemental composition and the oxide layer percentage on the surface of the GaN films after CMP with the three abrasives were measured by the X-ray photoelectron spectroscopy (XPS) method. The friction between the slurry and the GaN, as well as the surface temperature of the polishing pad during the CMP process, were evaluated using the POLI-500 polisher from GnP Corporation. A schematic diagram of the POLI-500 polishing machine equipment is presented in Fig. 3, while the operating parameters are outlined in Table 4.

## 3. Results and discussion

### 3.1. Performance of three different abrasives in GaN CMP

In this study, firstly, the CMP experiments were carried out for each of the three abrasives with different solid concentration, and the MRR results are shown in Fig. 4(1). It is clear from this result that the MRR of  $SiO_2$  abrasives is always lower than that of  $Al_2O_3$  and  $CeO_2$ . The MRR of  $SiO_2$  and  $Al_2O_3$  have a similar trend. When the abrasive concentration is increased from 0.5 wt% to 2.0 wt%, the MRR increased. When the abrasive concentration continues to increase, the MRR is no longer increased or even decreased. For  $CeO_2$  slurries, the MRR varies less with increasing abrasive concentration and is consistently in the range of 240–270 nm/h. At a  $CeO_2$  concentration of 2.0 wt%, the MRR reaches a maximum of 265.3 nm/h. In addition to this,  $Al_2O_3$  and  $SiO_2$  reached the highest values of MRR ( $Al_2O_3$  242.4 nm/h,  $SiO_2$  74.5 nm/h) at concentrations of 2.0 and 3.0, respectively. When the concentration of the

**Table 4**  
Parameters of the POLI-500 polisher.

Parameter	Unit	Value
Head pressure	g/cm <sup>2</sup>	250
Ring pressure	g/cm <sup>2</sup>	350
Polishing time	min	5
Slurry flow rate	ml/min	100
Pad rotation speed	rpm	50
Head rotation speed	rpm	50

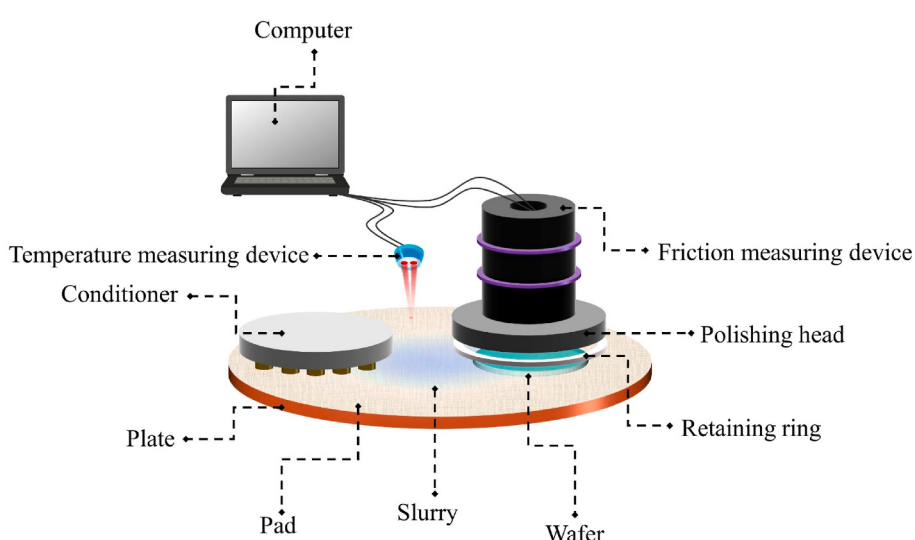


**Fig. 3.** Schematic diagram of the friction and polishing pad surface temperature measurement equipment.

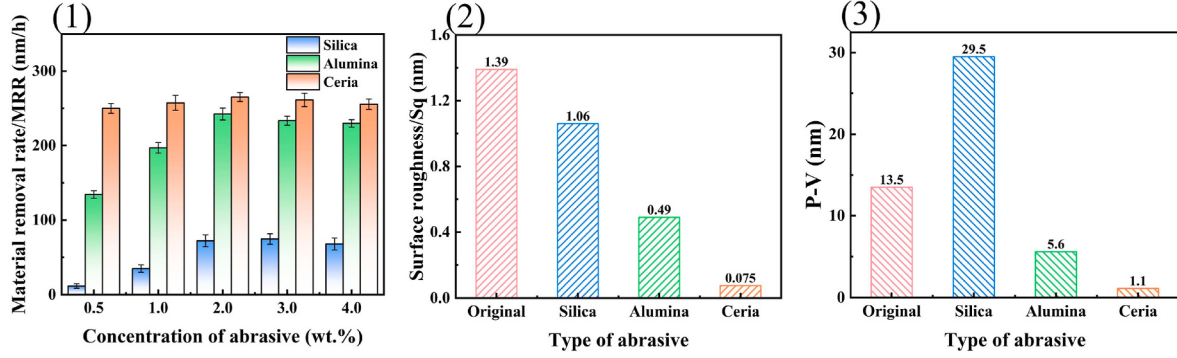


Fig. 4. The polishing results corresponding to three types of abrasives: (1) MRR, (2) Sq, (3) P-V.

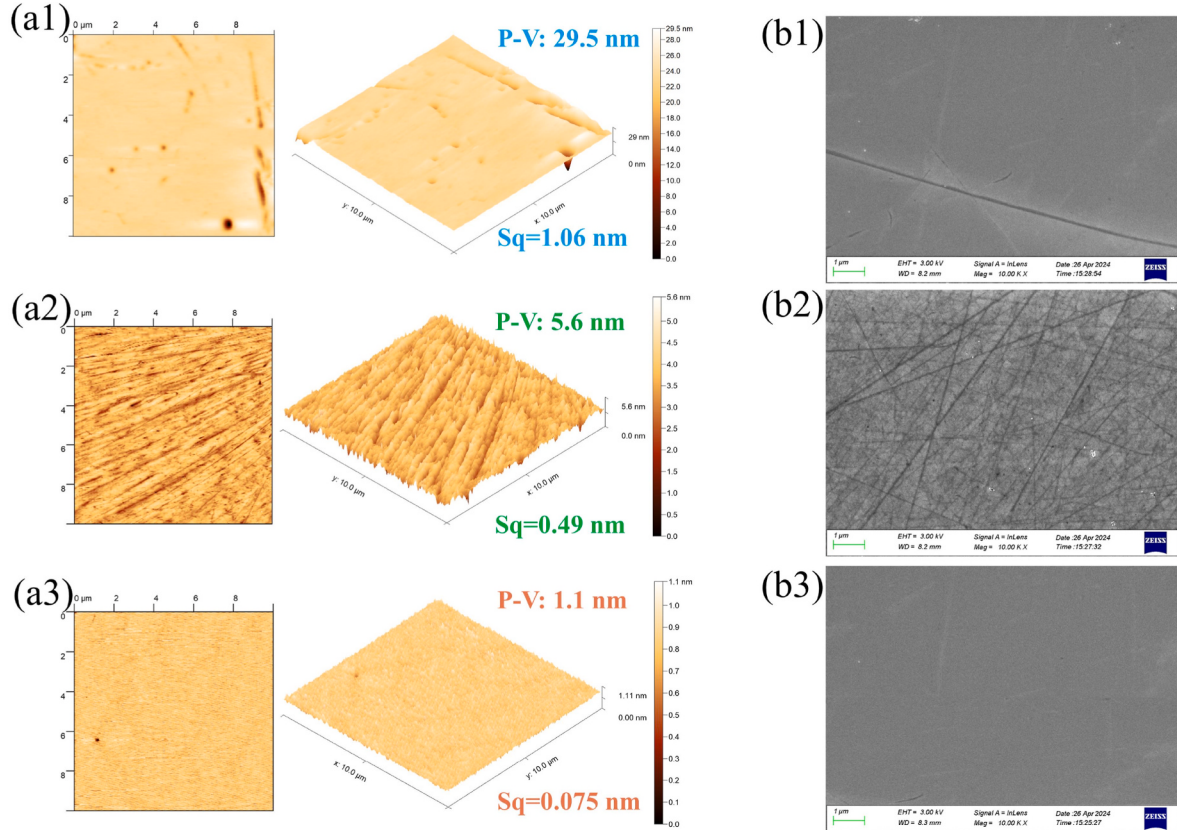


Fig. 5. The surface morphology of GaN after polishing with three types of abrasives. (a1) ~ (a3) are images measured by AFM, and (b1) ~ (b3) are images measured by SEM. (a1) and (b1) are surfaces polished with the SiO<sub>2</sub>-based slurry, (a2) and (b2) correspond to Al<sub>2</sub>O<sub>3</sub>-based slurry, and (a3) and (b3) are CeO<sub>2</sub>-based slurry.

three slurries is 2.0 wt%, the corresponding MRR is very high. Therefore, the surface morphology and roughness of GaN surfaces polished was measured under this concentration condition. It has been pointed out in some studies that the P-V value can also reflect the surface quality of the material surface to some extent [24,25]. The smaller the P-V value, the lower the degree of high and low undulation of the surface, and the smoother that surface is. From Fig. 4 (2) and (3), it can be seen that the Sq (0.075 nm) and P-V (1.1 nm) of the GaN surface polished with CeO<sub>2</sub>-based slurry are the lowest. The Sq (1.06 nm) and P-V (29.5 nm) of the surface polished with SiO<sub>2</sub>-based slurry are the highest. From Fig. 4 (2) and (3), it can be seen that the Sq and P-V of the GaN surface polished with CeO<sub>2</sub>-based slurry are the lowest among the three sets of surfaces. The surface polished with SiO<sub>2</sub>-based slurry has the highest Sq (1.06 nm) and P-V (29.5 nm). It was demonstrated in the study by Xiaolei Shi et al. that the height of the GaN atomic step-terrace is around 1 nm [26]. This

means that the P-V value of the GaN surface is always larger than 1 nm. The theoretical limit for the Sq of the GaN surface is 0.064 nm [27]. Therefore, the values of Sq and P-V for the surface after polishing with CeO<sub>2</sub>-based slurry are very close to their theoretical limits.

From the AFM images in Fig. 5, it can be observed that the surface polished with CeO<sub>2</sub>-based slurry is very smooth. In contrast, the surface polished using SiO<sub>2</sub>-based slurry demonstrates superior morphological characteristics compared to that polished with Al<sub>2</sub>O<sub>3</sub>-based slurry. This distinction arises from the presence of dense, elongated scratches on the alumina-polished surface, whereas the silica-polished surface features merely scattered pits. This distinction can be observed more clearly observed from the SEM images in Fig. 5. It is well-established that scratches on the GaN surface can be observed more clearly using an optical microscope according to Hideo Aida et al. [28,29].

In order to more accurately assess the surface quality of GaN, the

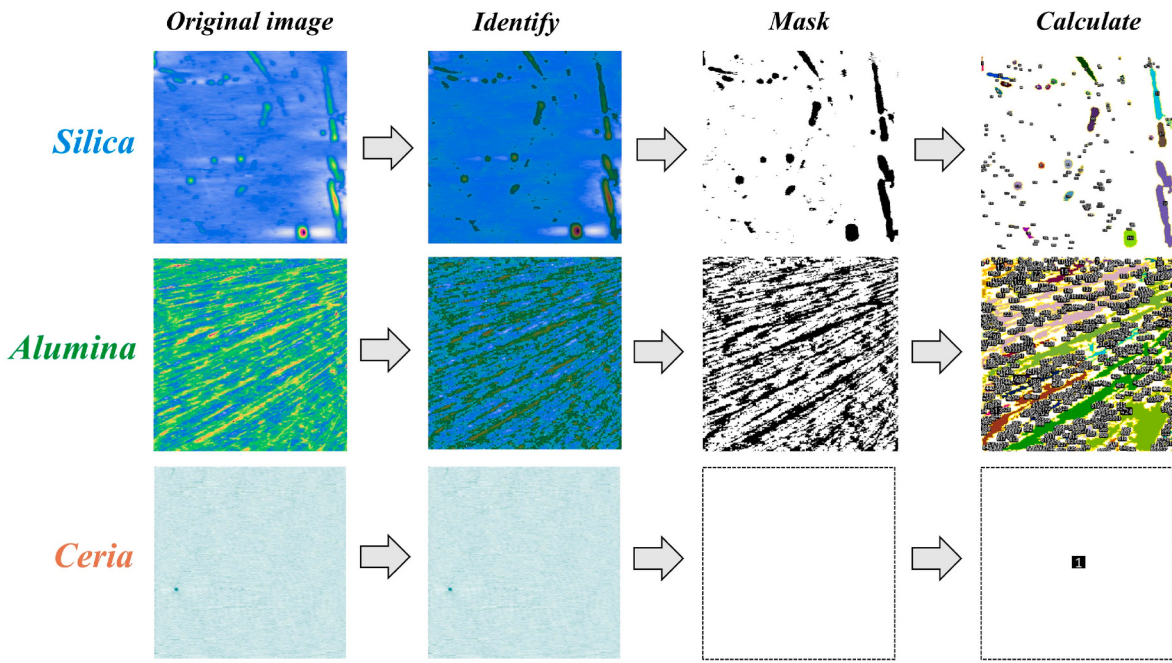


**Fig. 6.** Measurement method of the percentage of the surface defect area based on the AFM images.

**Table 5**

Percentage of defective areas of the surfaces treated with different types of slurry.

Type of abrasive	Percentage of defective area
Silica	7.1 %
Alumina	42.3 %
Ceria	0 %

percentage of surface defect area was introduced in this study. This index was mentioned in our previous study [30], and the specific calculation method is shown in Eq. (2):

$$r_a = \frac{S_d}{S_m} \times 100\% \quad (2)$$

where  $S_d$  is the area of the defective area in the measurement range and  $S_m$  is the total measurement area. This study utilized the software of “Gwyddion” and “ImageJ” to identify, mark, and calculate the area of defect regions in AFM images. In this study, regions with depressions exceeding 5 nm were defined as defect areas. Fig. 6 shows the image processing procedure for identifying and calculating the defect areas corresponding to silica and alumina. The final calculation results are presented in Table 5. It is evident that the percentage of the defective area on the GaN surface treated with an  $\text{Al}_2\text{O}_3$ -based slurry is significantly higher than that of surfaces treated with the other two slurries. Moreover, these data also indicate that the GaN surface treated with  $\text{CeO}_2$ -based slurry performs excellently, achieving superior performance on all three surface quality evaluation metrics.

GaN thin films exhibit a stepped structure, typically linked to the high-quality growth of crystals. This particular configuration enhances the photovoltaic conversion efficiency of the device by boosting light absorption and facilitating the effective separation and transport of charge carriers [7]. Consequently, the preservation of the atomic step-terrace morphology on the surface of polished GaN films serves as a critical indicator for assessing the surface quality of GaN post-CMP. From Fig. 7, it can be seen that the atomic step-terrace morphology of the GaN surface after polishing with  $\text{CeO}_2$ -based slurry. It can be observed that not only complete GaN atomic step-terraces can be measured on this surface but also the dislocation areas left during the

growth of the GaN film can be seen. This indicates that the GaN surface treated with ceria has truly achieved ultra-smoothness at the atomic scale.

To further investigate the impact of the three abrasives on the surface of GaN during the aforementioned polishing experiments, this study proceeded to assess the surface quality and roughness of the polished wafers. To ensure the reliability of the measurements, assessments were conducted at three distinct points on the wafer surface, with the precise assessment locations depicted in Fig. 8 (f). The morphology and surface roughness, as determined by AFM, are also depicted in Fig. 8. From Fig. 8(a)–(c), it is evident that the surface polished with ceria slurry exhibits the highest quality. The surface treated with ceria slurry lacks long scratches and large, deep pits. Furthermore, regardless of whether we consider the  $\text{Sq}$  or  $\text{P-V}$  values, these parameters are the lowest for the ceria slurry among the three different slurries tested. The three-point measurement results indicate that the impact of the three abrasives on the GaN surface aligns with the findings of the aforementioned experiments.

### 3.2. Mechanism analysis

In this study, the three abrasives differ not only in hardness but also in their micro-morphology. The micro-morphology of the three abrasives is shown in Fig. 9. Based on this, it is inferred that the friction behavior between one of the three abrasives and the GaN surface during the CMP process will be significantly different. Fig. 9 (4) is a schematic diagram of the friction process between one of the three abrasives and the GaN surface during the CMP process. Some previous research indicated that, under identical conditions, the frictional forces between two rigid bodies are generally less than those between non-rigid bodies [31, 32]. Given that the hardness of silica and GaN is relatively similar, it is postulated that the frictional interaction between silica abrasives and GaN would approximate that of two rigid bodies. The friction between spherical structured silica and the GaN surface will be further reduced. For ceria and alumina, their friction with GaN is closer to non-rigid body friction. Therefore, during the friction process, the abrasive may deform against the GaN surface, increasing the friction force during the polishing process. From Fig. 9 (4), it is evident that ceria abrasives with lower hardness are prone to deformation during the friction process,

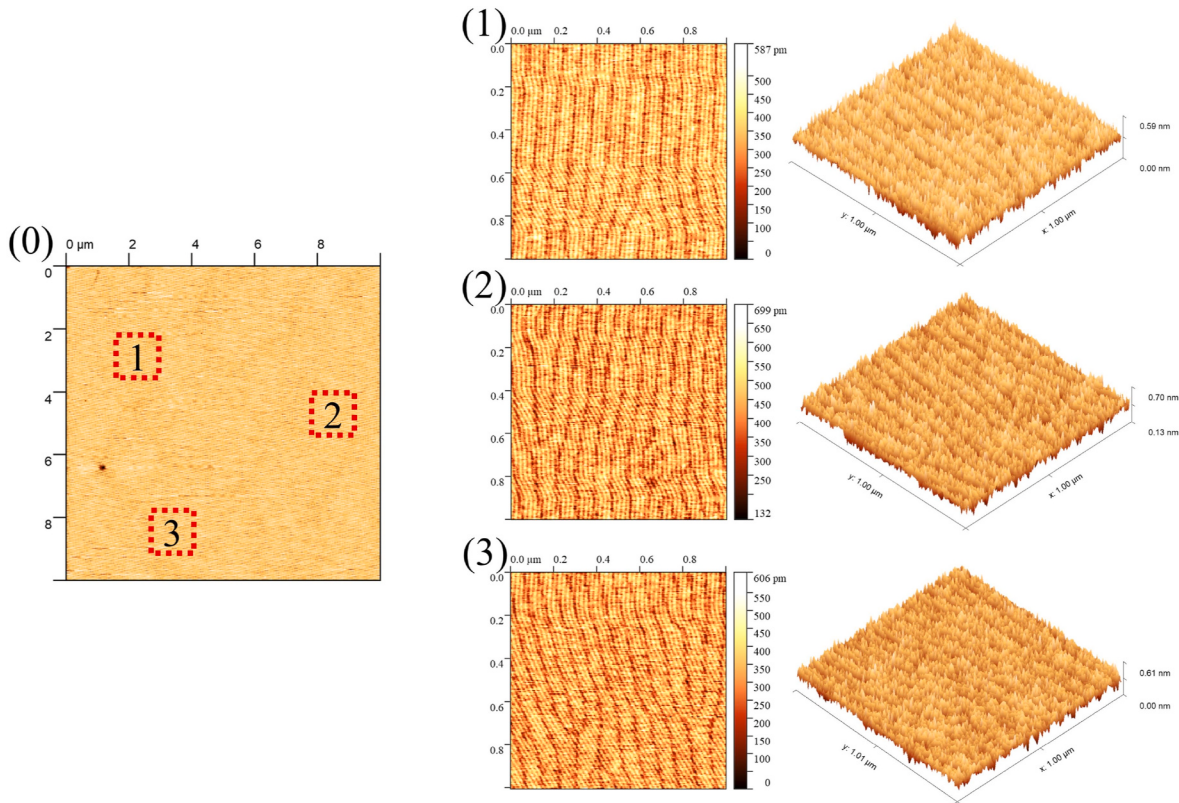


**Fig. 7.** Atomic step-terrace morphology of the GaN surface treated with CeO<sub>2</sub>-based slurry. (0) indicates the measurement site of the atomic steps, while (1), (2), and (3) represent the atomic step-terrace morphologies within three different measurement areas.

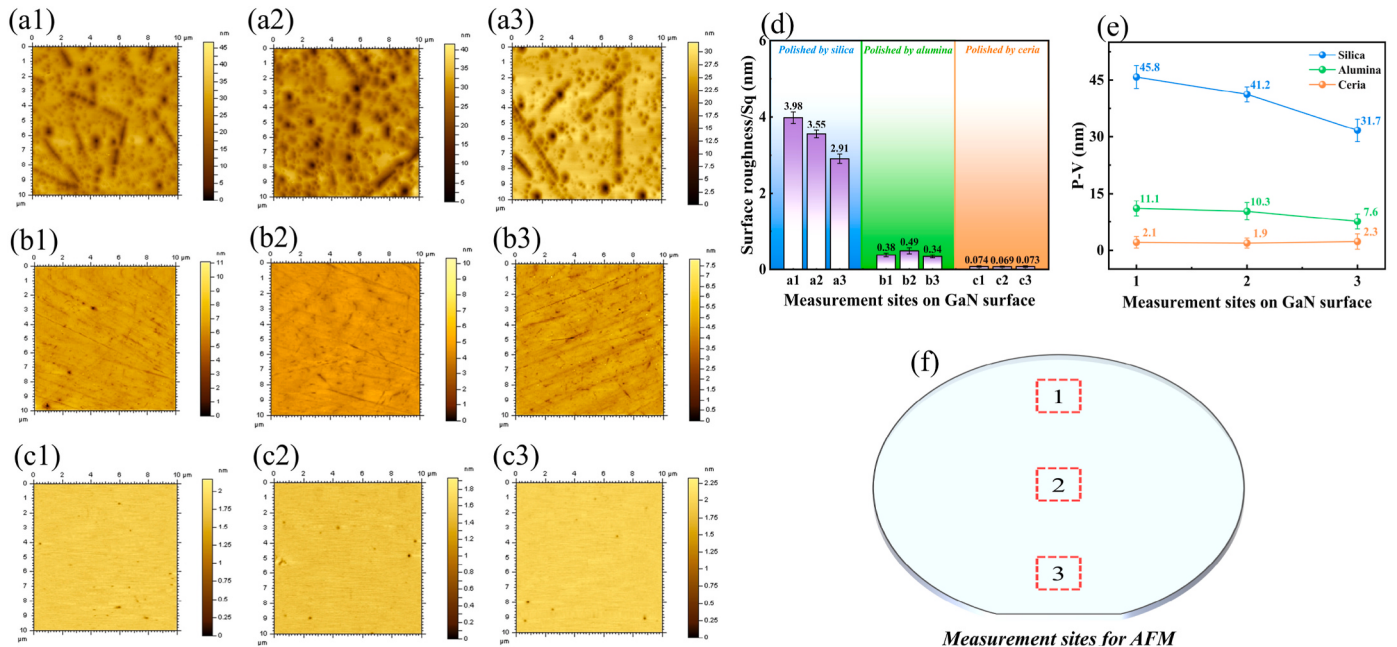


**Fig. 8.** GaN surface morphology after CMP for 10 min using three abrasives. (a1) ~ (a3) polished by silica slurry, (b1) ~ (b3) polished by alumina slurry, (c1) ~ (c3) polished by ceria slurry. (1) Schematic diagram of the measurement site, (d)  $S_q$  corresponding to the three abrasives, (e) P-V corresponding to the three abrasives. (f) AFM measurement sites on the GaN surface.

which in turn increases the friction force. Conversely, alumina abrasives, which possess a hardness exceeding that of GaN, may not undergo deformation due to the frictional forces exerted by GaN during CMP. In conclusion, it is challenging to ascertain which abrasive will exhibit the

greatest frictional interaction with GaN based solely on the hardness of abrasives and micro-morphology.

This investigation employed the POLI-500 polisher to measure the COF between the slurries associated with the three abrasives and the

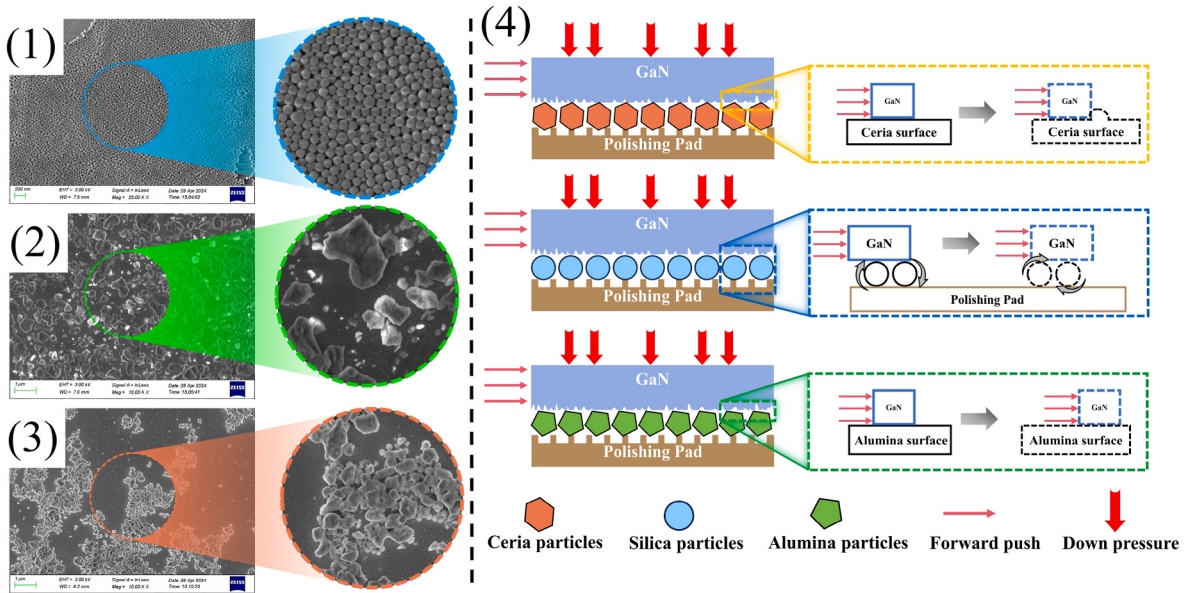


**Fig. 9.** The micromorphology of the three different abrasives: (1) silica, (2) alumina, and (3) ceria. (4) A schematic diagram of the friction process between the three abrasives and the surface of GaN.

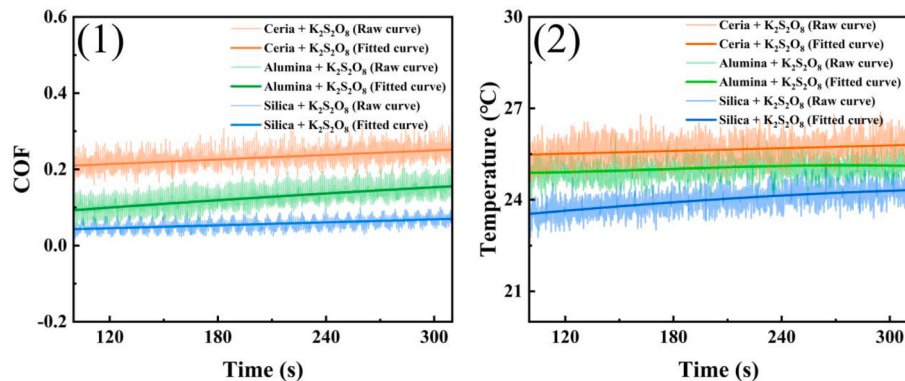


**Fig. 10.** The COF between three types of slurries and the surface of GaN (1), and the surface temperature of the polishing pad during CMP (2).

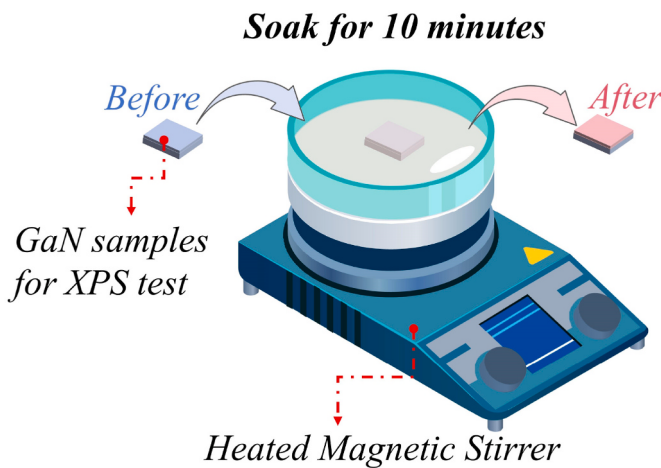


**Fig. 11.** Schematic diagram of the XPS validation experiments for mechanistic analysis.

GaN surface. Concurrently, it monitored the surface temperature of the polishing pad throughout the process. To enhance the clarity of the distinctions among the measurement outcomes, the raw COF and temperature data were subjected to real-time fitting with their respective average values. The fitted equation is given in Eq. (3):

$$y = y_0 + A_1 \times \exp(- (x - x_0) / t_0) \quad (3)$$

where  $y_0$  is offset,  $x_0$  is center,  $A_1$  is amplitude, and  $t_0$  is the time constant. Both the fitted curves and the unprocessed data are presented in Fig. 10. The measurement results of the COF indicate that the COF between the CeO<sub>2</sub>-based slurry and the GaN surface is significantly higher than that of slurries containing the other two abrasives. This outcome proves the hypothesis regarding the frictional behavior between one of three abrasives and the GaN surface, as depicted in Fig. 9 (4) of this study. It is noteworthy that during polishing with CeO<sub>2</sub>-based slurry, the surface temperature of the polishing pad remains the highest as well. According to the Arrhenius equation, as shown in Eq. (3), it can be seen that the higher the temperature the faster the rate of the chemical reaction,

$$k = Ae^{-\frac{E_a}{RT}} \quad (4)$$

where  $k$  is the rate constant (frequency of collisions resulting in a reaction),  $A$  is the pre-exponential factor,  $E_a$  is the apparent activation

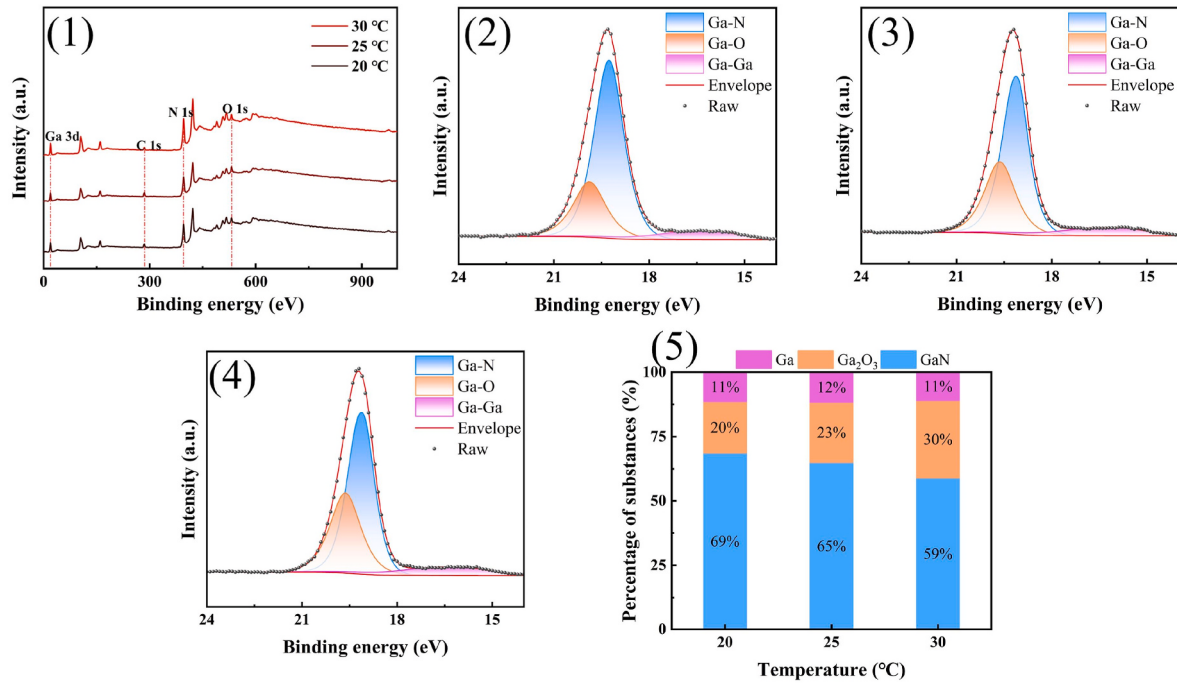


**Fig. 12.** (1) XPS test results of elements on the polished GaN surface. Ga 3d spectra and the content of different substances on the surface of GaN samples at different temperatures. (2) 20 °C, (3) 25 °C, (4) 30 °C, (5) the content of different substances.

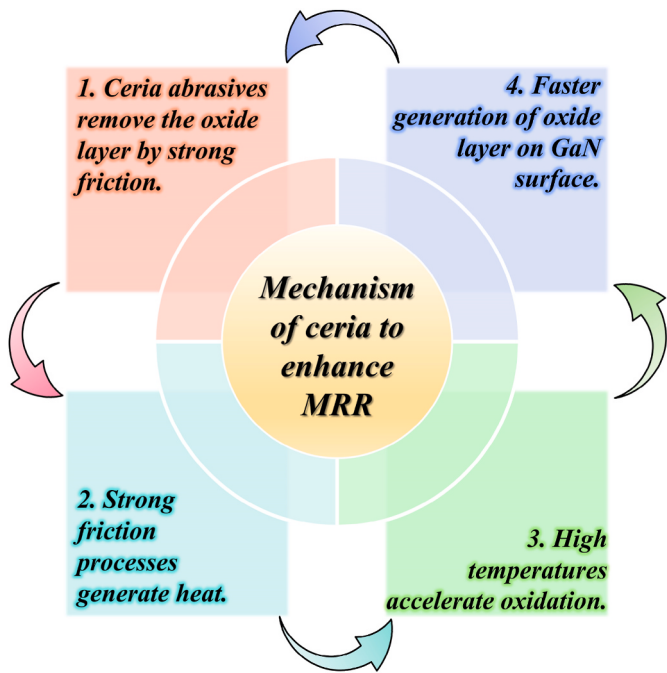


**Fig. 13.** The mechanism of CeO<sub>2</sub>-based slurry enhancing MRR.

energy,  $R$  is the universal gas constant ( $8.314 \text{ J mol}^{-1} \text{ K}^{-1}$ ), and  $T$  is the absolute temperature [33,34]. In this study, the chemical reactions that would be present in the CMP process are shown in Eqs. (5)–(7) [35,36]. In particular, according to Eq. (5), the stronger the friction and the more heat is generated in GaN CMP, the faster  $\text{SO}_4^{2-}$  is generated. This will substantially increase the oxidation rate of the slurry on the GaN surface. The high chemical reaction rate and the strong mechanical friction result in the high MRR of CeO<sub>2</sub>-based slurry. In summary, for CeO<sub>2</sub>-based slurry, the maximum friction and the highest surface temperature of the polishing pad in CMP are the main factors for having the highest MRR.

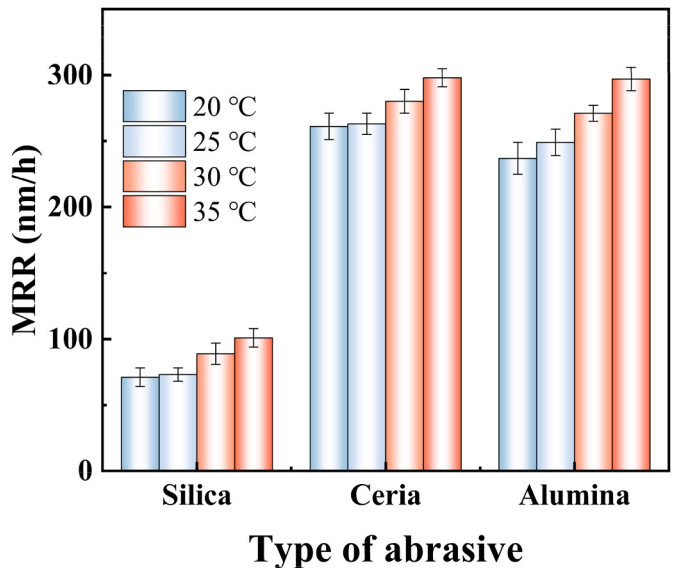


**Fig. 14.** The mechanism of CeO<sub>2</sub>-based slurry enhancing MRR.



To substantiate the hypothesis that CeO<sub>2</sub>-based slurries increase the MRR, XPS was used for further investigation. The preparation of samples for XPS analysis is depicted in Fig. 11. GaN samples were submerged in a potassium persulfate solution (with a concentration of 2.0 wt% K<sub>2</sub>S<sub>2</sub>O<sub>8</sub>) at varying temperatures for a duration of 10 min. It is used to simulate the oxidation process of GaN at different temperatures during the CMP process. The temperature of the potassium persulfate solution is set to

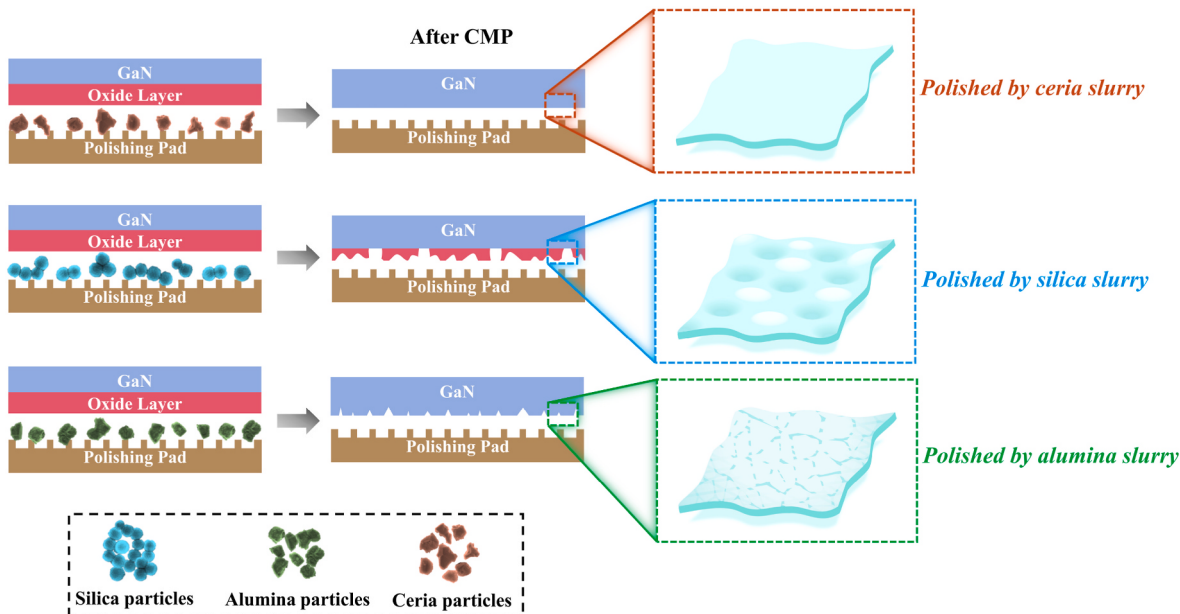


**Fig. 15.** Schematic diagram of the effect of three different hardness of abrasives on the GaN surface morphology during the CMP process.

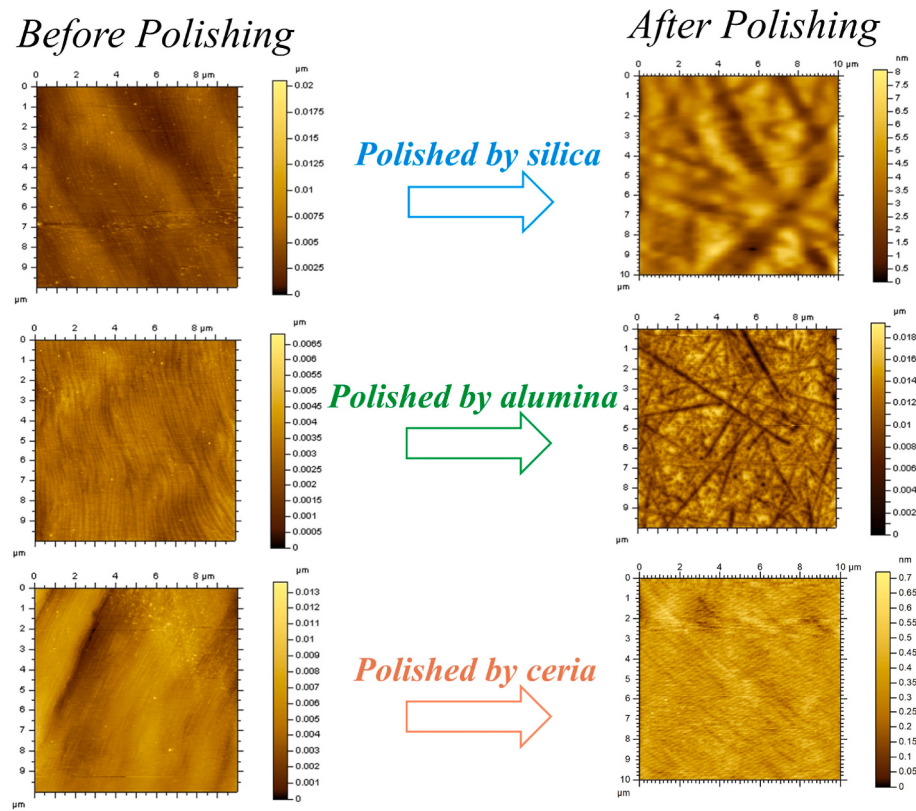


**Fig. 16.** Surface morphology of GaN after grinding with the three abrasives.

20 °C, 25 °C, and 30 °C, respectively. Fig. 12 illustrates the results of the XPS measurements, revealing that as the temperature of the potassium persulfate solution increases, there is a corresponding rise in the Ga-O content on the surface of GaN. Some studies suggested a direct correlation between the Ga-O content and the thickness of the oxide layer on the surface of GaN, indicating that a higher Ga-O content results in a thicker oxide layer [37–41]. This indicates that within the same immersion time, the oxidation rate of the GaN surface in potassium

persulfate solution at 30 °C is the fastest. Therefore, it is clear that the surface temperature of the polishing pad during the GaN CMP process directly affects the oxidation of GaN by potassium persulfate, with higher temperatures leading to a faster oxidation rate of GaN.

In summary, the mechanism by which CeO<sub>2</sub>-based slurries significantly enhance the MRR is proposed as: Firstly, during the CMP process, there is a strong frictional interaction between ceria and the surface of GaN, which continuously increases the temperature of the polishing pad

surface. Secondly, the rising temperature accelerates the oxidation of the GaN surface by potassium persulfate, and the rapidly formed oxide layer is subsequently removed by the strong frictional action of ceria particles [42,43]. This process repeated occurs throughout the entire GaN CMP, ultimately leading to a significant improvement in MRR. The CMP mechanism in CeO<sub>2</sub>-based slurry system is shown in Fig. 13.

To further verify the importance of temperature for polishing efficiency, the control experiments were carried out. The slurry was heated to different temperature before polishing. The MRR results are shown in Fig. 14, it is found that the MRR of all three abrasives increases with increasing temperature. In particular, the MRR of alumina and ceria are basically close to each other when the temperature of the slurry is raised to 35 °C. These polishing results are consistent with the XPS results. Nevertheless, the MRR associated with silica slurry remains at a low level. This suggests that even in the presence of a strong chemical reaction, reduced friction can also diminish the efficiency of the polishing process.

For GaN CMP, the presence of an oxide layer can protect the underlying smooth surface from excessive abrasion by the abrasives. However, based on the experimental results of this study, we hypothesize that if the oxide layer generated on the GaN surface is not removed in a timely manner, it will also result in poor surface quality of GaN. The study posits that the mechanism by which three different abrasives affect the surface of GaN is depicted in Fig. 15. The increased P-V value observed in the SiO<sub>2</sub>-polished surface, in comparison to the untreated surface, may be attributed to uneven material removal. This could result from the larger particle size or distinct interaction mechanisms between the abrasive and the GaN surface. Such variations in the polishing process may produce more pronounced surface peaks and valleys, consequently leading to a higher P-V value. It is proposed that ceria can rapidly eliminate the oxide layer on the GaN surface without causing damage to the underlying GaN. In contrast, alumina swiftly strips away the oxide layer but continues to degrade the GaN surface. Furthermore, silica abrasive exhibits a notably low efficacy in removing the oxide layer, and even upon completion of CMP, it fails to fully eliminate the oxide layer, ultimately leading to a surface with high roughness.

To validate the aforementioned mechanism, the GaN were polished using three different types of abrasives in this study and subsequently observed the surface morphology post-polishing, utilizing AFM for analysis. Fig. 16 illustrates the corresponding AFM measurement images. It is worth noting that the slurry contained only 2.0 wt% abrasive, with the pH adjusted to 3.0 using nitric acid. The polishing time is 10 min. From Fig. 16, it becomes evident that the GaN surface, after being ground with alumina abrasive, exhibits numerous pronounced scratches. In contrast, the surface ground with silica abrasive lacks such visible scratches, yet it displays several darkened regions. Referencing the color scale positioned on the image's right side, these darkened areas correspond to pits approximately 8 nm in depth. When comparing the surface ground with ceria abrasive to the initial surface, it is apparent that no additional scratches or pits have been introduced. Therefore, mechanical friction between the ceria abrasive and the GaN surface does not cause any damage to the GaN surface. In summary, during the CMP process, the strong mechanical friction between ceria abrasives and GaN not only promotes the generation of an oxide layer, significantly increasing the MRR but also does not damage the smooth surface of the underlying GaN. This is the main reason for the excellent performance of ceria abrasives in GaN CMP.

#### 4. Conclusion

This research highlights the superior efficiency of ceria-based slurry in GaN CMP, achieving the highest MRR of 265.3 nm/h and the lowest surface roughness ( $S_q = 0.075$  nm). The study elucidates that the enhanced CMP performance is due to the strong frictional interaction and heat generation during polishing, facilitating rapid oxidation of GaN and effective material removal without surface damage. The findings

provide valuable insights for optimizing CMP processes for GaN-based devices, indicating ceria-based slurries as a promising option for improving CMP efficiency and GaN surface quality.

#### CRediT authorship contribution statement

**Wen-hao Xian:** Writing – original draft, Methodology, Investigation, Formal analysis. **Baoguo Zhang:** Investigation, Funding acquisition, Formal analysis. **Shitong Liu:** Writing – review & editing, Supervision, Data curation. **Yijun Wang:** Investigation, Data curation. **Sihui Qin:** Investigation. **Yang Liu:** Investigation.

#### Declaration of competing interest

The authors declare that they have no known competing financial interests or personal relationships that could have appeared to influence the work reported in this paper.

#### Acknowledgments

This work was supported by the One Hundred Talent Project of Hebei Province of China (E2013100006).

#### Data availability

No data was used for the research described in the article.

#### References

- [1] M. Meneghini, C. De Santi, I. Abid, M. Buffolo, M. Cioni, R.A. Khadar, L. Nela, N. Zagni, A. Chini, F. Medjdoub, G. Meneghesso, G. Verzellesi, E. Zanoni, E. Matioli, GaN-based power devices: physics, reliability, and perspectives, *J. Appl. Phys.* 130 (2021) 181101, <https://doi.org/10.1063/5.0061354>.
- [2] T. Hashimoto, E.R. Letts, D. Key, Progress in near-equilibrium ammonothermal (NEAT) growth of GaN substrates for GaN-on-GaN semiconductor devices, *Crystals* 12 (2022) 1085, <https://doi.org/10.3390/cryst12081085>.
- [3] Q. Jiang, C. Liu, Y. Lu, K.J. Chen, 1.4-kV AlGaN/GaN HEMTs on a GaN-on-SOI platform, *IEEE Electron. Device Lett.* 34 (2013) 357–359, <https://doi.org/10.1109/LED.2012.2236637>.
- [4] H.D. Jabbar, M.A. Fakhri, M. Jalal AbdulRazzaq, Gallium nitride -based photodiode: a review, *Mater. Today Proc.* 42 (2021) 2829–2834, <https://doi.org/10.1016/j.matpr.2020.12.729>.
- [5] F.K. Yam, L.L. Low, S.A. Oh, Z. Hassan, F.K. Yam, L.L. Low, S.A. Oh, Z. Hassan, Gallium nitride: an overview of structural defects, in: *Optoelectron. - Mater. Tech.*, IntechOpen, 2011, <https://doi.org/10.5772/19878>.
- [6] B. Shen, N. Tang, X.-L. Yang, M.-J. Wang, F.-J. Xu, X.-Q. Wang, Z.-X. Qin, Study of the epitaxial growth, physical properties and electronic devices of GaN-based semiconductor heterostructures, *Prog. Phys.* 37 (2017) 81–97, <https://doi.org/10.13725/j.cnki.pip.2017.03.001>.
- [7] Y. Pal, M. Anthony Raja, M. Madhumitha, A. Nikita, A. Neethu, Fabrication and characterization of gallium nitride thin film deposited on a sapphire substrate for photoelectrochemical water splitting applications, *Optik* 226 (2021) 165410, <https://doi.org/10.1016/j.jileo.2020.165410>.
- [8] B. Guo, G. Yu, L. Zhang, J. Zhou, Z. Wang, R. Xing, A. Yang, Y. Li, B. Liu, X. Zeng, Z. Du, X. Deng, Z. Zeng, B. Zhang, High-performance N-polar GaN/alGaN metal-insulator-semiconductor high-electron-mobility transistors with low surface roughness enabled by chemical-mechanical-polishing-incorporated layer transfer Technology, *Crystals* 14 (2024) 253, <https://doi.org/10.3390/cryst14030253>.
- [9] L.-W. Ou, Y.-H. Wang, H.-Q. Hu, L.-L. Zhang, Z.-G. Dong, R.-K. Kang, D.-M. Guo, K. Shi, Photochemically combined mechanical polishing of N-type gallium nitride wafer in high efficiency, *Precis. Eng.* 55 (2019) 14–21, <https://doi.org/10.1016/j.precisioneng.2018.08.002>.
- [10] X. Yu, B. Zhang, R. Wang, Z. Kao, S. Yang, W. Wei, Effect of photocatalysts on electrochemical properties and chemical mechanical polishing rate of GaN, *Mater. Sci. Semicond. Process.* 121 (2021) 105387, <https://doi.org/10.1016/j.mssp.2020.105387>.
- [11] Z. Ni, S. Zheng, G. Chen, Q. Fan, X. Zhang, H. Zhang, J. Li, D. Bian, S. Qian, Enhancement mechanism of chemical mechanical polishing for GaN based on electro-fenton reaction, *ECS J. Solid State Sci. Technol.* 12 (2023) 024005, <https://doi.org/10.1149/2162-8777/ab736>.
- [12] Q. Zheng, J. Pan, R. Zhou, Z. Zhuo, Q. Yan, Mechanism of electrochemically assisted friction and wear behavior of GaN in KMnO<sub>4</sub> slurry, *ECS J. Solid State Sci. Technol.* 12 (2023) 074008, <https://doi.org/10.1149/2162-8777/ace7c3>.
- [13] C. Ke, S. Liu, Y. Pang, Y. Wei, Y. Wu, Q. Luo, Y. Wu, J. Lu, Synergistic effect of abrasive friction and glycine on improving chemical mechanical polishing performance of single-crystal GaN substrate, *Ceram. Int.* 50 (2024) 21357–21366, <https://doi.org/10.1016/j.ceramint.2024.03.247>.

- [14] Q. Li, L. Liu, J. Yu, S. Wang, G. Wang, Z. Wang, Z. Qi, X. Zhao, G. Liu, X. Xu, L. Zhang, Investigation on chemical mechanical polishing of Ga-faced GaN crystal with weak alkaline slurry, *Appl. Surf. Sci.* 653 (2024) 159396, <https://doi.org/10.1016/j.apsusc.2024.159396>.
- [15] J. Pan, Y. Wu, Z. Zhuo, H. Wang, Q. Zheng, Q. Yan, Experimental study of single-crystal GaN wafer electro-Fenton magnetorheological complex friction wear, *Tribol. Int.* 180 (2023) 108260, <https://doi.org/10.1016/j.triboint.2023.108260>.
- [16] J. Pan, Z. Zhuo, Q. Zhang, Q. Zheng, Q. Yan, Friction and wear mechanisms for single crystal GaN based on an electro-Fenton enhanced chemical reaction, *Wear* (2022) 498–499, <https://doi.org/10.1016/j.wear.2022.204315>, 204315.
- [17] H. Guan, S. Niu, Y. Wang, X. Lu, Z. Ding, W. Liu, D. Zhao, Synergetic effect of  $H_2O_2$  and PTA on the microscratch and indentation of GaN wafer with electricity, *Tribol. Int.* 158 (2021) 106941, <https://doi.org/10.1016/j.triboint.2021.106941>.
- [18] C. Zou, G. Pan, X. Shi, H. Gong, Y. Zhou, Atomically smooth gallium nitride surface prepared by chemical-mechanical polishing with different abrasives, *Proc. Inst. Mech. Eng. Part J J. Eng. Tribol.* 228 (2014) 1144–1150, <https://doi.org/10.1177/1350650114535383>.
- [19] W. Wei, B. Zhang, L. Zhang, X. Yu, Study on electrochemical corrosion and CMP of GaN in different oxidation systems, *ECS J. Solid State Sci. Technol.* 11 (2022) 034002, <https://doi.org/10.1149/2162-8777/ac5807>.
- [20] W. Wang, B. Zhang, Y. Shi, J. Zhou, R. Wang, N. Zeng, Improved chemical mechanical polishing performance in 4H-SiC substrate by combining novel mixed abrasive slurry and photocatalytic effect, *Appl. Surf. Sci.* 575 (2022) 151676, <https://doi.org/10.1016/j.apsusc.2021.151676>.
- [21] W. Wang, B. Zhang, Y. Shi, T. Ma, J. Zhou, R. Wang, H. Wang, N. Zeng, Improvement in chemical mechanical polishing of 4H-SiC wafer by activating persulfate through the synergistic effect of UV and  $TiO_2$ , *J. Mater. Process. Technol.* 295 (2021) 117150, <https://doi.org/10.1016/j.jmatprotec.2021.117150>.
- [22] W. Ye, Z. Baoguo, W. Pengfei, L. Min, C. Dexing, X. Wenhao, Improving the dispersion stability and chemical mechanical polishing performance of  $CeO_2$  slurries, *ECS J. Solid State Sci. Technol.* 12 (2023) 044004, <https://doi.org/10.1149/2162-8777/accaa5>.
- [23] M. Liu, B. Zhang, J. Seo, W. Xian, D. Cui, S. Liu, Y. Wang, S. Qin, Y. Liu, Development of Highly stable ceria slurry in acetic acid-ammonium acetate buffer Media for effective chemical mechanical polishing of silicon dioxide, *Mater. Sci. Semicond. Process.* 177 (2024) 108411, <https://doi.org/10.1016/j.mssp.2024.108411>.
- [24] H. Deng, K. Endo, K. Yamamura, Atomic-scale and pit-free flattening of GaN by combination of plasma pretreatment and time-controlled chemical mechanical polishing, *Appl. Phys. Lett.* 107 (2015) 051602, <https://doi.org/10.1063/1.4928195>.
- [25] D. Toh, K. Kayao, R. Ohnishi, A.I. Osaka, K. Yamauchi, Y. Sano, Bias-assisted photoelectrochemical planarization of GaN (0001) with impurity concentration distribution, *AIP Adv.* 13 (2023) 095113, <https://doi.org/10.1063/5.0151387>.
- [26] X. Shi, C. Zou, G. Pan, H. Gong, L. Xu, Y. Zhou, Atomically smooth gallium nitride surface prepared by chemical-mechanical polishing with  $S_2O_8^{2-}/Fe^{2+}$  based slurry, *Tribol. Int.* 110 (2017) 441–450, <https://doi.org/10.1016/j.triboint.2016.09.037>.
- [27] H. Aida, T. Doi, H. Takeda, H. Katakura, S.-W. Kim, K. Koyama, T. Yamazaki, M. Uneda, Ultraprecision CMP for sapphire, GaN, and SiC for advanced optoelectronics materials, *Curr. Appl. Phys.* 12 (2012) S41–S46, <https://doi.org/10.1016/j.cap.2012.02.016>.
- [28] H. Aida, H. Takeda, N. Omiya, T. Doi, Rapid estimation of removal rate of chemical mechanical polishing of gallium nitride substrate by quantitative diagnosis of cathodoluminescence images, *ECS J. Solid State Sci. Technol.* 10 (2021) 106007, <https://doi.org/10.1149/2162-8777/ac210c>.
- [29] H. Aida, H. Takeda, T. Doi, Analysis of mechanically induced subsurface damage and its removal by chemical mechanical polishing for gallium nitride substrate, *Precis. Eng.* 67 (2021) 350–358, <https://doi.org/10.1016/j.precisioneng.2020.10.007>.
- [30] W. Xian, B. Zhang, M. Liu, P. Wu, Y. Wang, S. Liu, D. Cui, Optimization and mechanism of  $SiO_2$ -based slurry components for atomically smooth gallium nitride surface obtained using chemical mechanical polishing technique, *ECS J. Solid State Sci. Technol.* 13 (2024) 014003, <https://doi.org/10.1149/2162-8777/ad1c89>.
- [31] D.E. Stewart, Rigid-body dynamics with friction and impact, *SIAM Rev.* 42 (2000) 3–39, <https://doi.org/10.1137/S0036144599360110>.
- [32] Rigid body collisions with friction, *Proc. R. Soc. Lond. Ser. Math. Phys. Sci.* (1990), <https://doi.org/10.1098/rspa.1990.0125>.
- [33] J. Crapse, N. Pappireddi, M. Gupta, S.Y. Shvartsman, E. Wieschaus, M. Wühr, Evaluating the Arrhenius equation for developmental processes, *Mol. Syst. Biol.* 17 (2021) e9895, <https://doi.org/10.15252/msb.20209895>.
- [34] M. Peleg, M.D. Normand, M.G. Corradini, The Arrhenius equation revisited, *Crit. Rev. Food Sci. Nutr.* 52 (2012) 830–851, <https://doi.org/10.1080/10408398.2012.667460>.
- [35] Y. Ji, C. Dong, D. Kong, J. Lu, Q. Zhou, Heat-activated persulfate oxidation of atrazine: implications for remediation of groundwater contaminated by herbicides, *Chem. Eng. J.* 263 (2015) 45–54, <https://doi.org/10.1016/j.cej.2014.10.097>.
- [36] D. Shi, W. Zhou, T. Zhao, Polishing of diamond, SiC, GaN based on the oxidation modification of hydroxyl radical: status, challenges and strategies, *Mater. Sci. Semicond. Process.* 166 (2023) 107737, <https://doi.org/10.1016/j.msspp.2023.107737>.
- [37] J. Wang, T. Wang, G. Pan, X. Lu, Mechanism of GaN CMP based on  $H_2O_2$  slurry combined with UV light, *ECS J. Solid State Sci. Technol.* 4 (2015) P112, <https://doi.org/10.1149/2.0191503jss>.
- [38] J. Guo, J. Gao, C. Xiao, L. Chen, L. Qian, Mechanochemical reactions of GaN-Al<sub>2</sub>O<sub>3</sub> interface at the nanasperity contact: roles of crystallographic polarity and ambient humidity, *Friction* 10 (2022) 1005–1018, <https://doi.org/10.1007/s40544-021-0501-9>.
- [39] R. Huang, T. Liu, Y. Zhao, Y. Zhu, Z. Huang, F. Li, J. Liu, L. Zhang, S. Zhang, A. Dingsun, H. Yang, Angular dependent XPS study of surface band bending on Ga-polar n-GaN, *Appl. Surf. Sci.* 440 (2018) 637–642, <https://doi.org/10.1016/j.apsusc.2018.01.196>.
- [40] L. Zhang, D. Lu, H. Deng, Study on material removal mechanisms in electrochemical etching-enhanced polishing of GaN, *J. Manuf. Process.* 73 (2022) 903–913, <https://doi.org/10.1016/j.jmapro.2021.11.059>.
- [41] Y. Zhu, X. Niu, Z. Hou, Y. Zhang, Y. Shi, R. Wang, Effect and mechanism of oxidant on alkaline chemical mechanical polishing of gallium nitride thin films, *Mater. Sci. Semicond. Process.* 138 (2022) 106272, <https://doi.org/10.1016/j.msspp.2021.106272>.
- [42] J. Deng, L.-F. Ren, L. Ma, C.-K. Lei, G.-M. Wei, W.-F. Wang, Effect of oxygen concentration on low-temperature exothermic oxidation of pulverized coal, *Thermochim. Acta* 667 (2018) 102–110, <https://doi.org/10.1016/j.tca.2018.07.012>.
- [43] Y. Yang, D. Xu, K. Zhang, Effect of nanostructures on the exothermic reaction and ignition of Al/CuOx based energetic materials, *J. Mater. Sci.* 47 (2012) 1296–1305, <https://doi.org/10.1007/s10853-011-5903-z>.